1991 Transactions
of NAMRI/SME

CONTROL OF RADIAL RUNOUT IN MULTI-TOOTH FACE MILLING

TSU-CHIN TSAO, Assistant Professor
KIN-CHEOK PONG, Graduate Student

Department of Mechanical and Industrial Engineering
University of Illinois at Urbana-Champaign

ABSTRACT

This paper investigates the feasibility of suppressing the effect of cutter runout on the maximum tangential cutting force in multi-tooth face milling by actively varying the spindle speed with a low inertia brushless DC motor drive. A dynamic model of an industrial direct spindle drive is derived and experimentally validated. A dynamic face milling model is developed to calculate the tangential cutting force under varying spindle speeds. The combination of the drive and machining dynamic models makes a comprehensive simulation model for variable speed face milling process. To suppress the uneven peak cutting forces generated by cutter radial runout, a special digital control algorithm, which is designed based on a discrete and simplified model of the comprehensive simulation model, is applied to vary the spindle speed in every cutter rotation. Simulation results show that the control system is effective in suppressing uneven chip loads at nominal spindle speeds lower than 500 rpm and is not effective at higher speeds due to the motor current saturation. In heavy cutting conditions such as large depth of cut and feed rate, it is shown that the control system design must consider another factor to ensure stability: the feedback from the cutting torque to the motor drive.

K_t	: tangential cutting force coefficient, N/m^2
K_u	: current loop PI controller gain, V/V
L_a	: armature inductance of the motor, H
Ln	: learning gain
N_t	: the cutter insert number
R	: nominal cutter radius, m
R_a	: armature resistance of the motor, W
T_{cut}	: cutting torque, N-m
T_e	: electrical torque, N-m
U_i*	: command spindle current in term of voltage, V
U_w*	: command spindle speed in term of voltage, V
v	: workpiece linear velocity in feed direction, m/s
v_o	: nominal feed speed, m/s
w	: spindle speed, rad/s
W_a	: spindle speed measured by tachometer, V
wid	: workpiece width, m
w_o	: nominal spindle speed, rad/s
x	: position of the cutter in feed direction with respect to the workpiece, m
$[A]$	: process state matrix
$[B]$	: process input matrix
$[C]$	: process output matrix
$[D]$	: disturbance input matrix
$\bar{x}$	: the states of the process
z^{-1}	: one step delay operator
Δ_i	: radial runout as seen by insert i, m
$\Delta\theta$	: insert spacing angle, rad
θ	: cutter angular displacement, rad
α_{in}	: cutting insert entry angle, rad
α_{out}	: cutting insert exit angle, rad
τ	: chip thickness, m
$\delta(\cdot)$	: variation of variable $\cdot$ from its nominal value

INTRODUCTION

Runout that occurs in rotational machinery has undesirable effects on machining systems. It causes each cutting insert to carry uneven chip loads, resulting in non-uniform cutting force patterns. Excessively large forces on a particular insert can damage or break the cutting tooth. Since the cutting force on each tooth is uneven, the teeth may be worn unevenly; this uneven wearing reduces the cutter life. Periodic peak forces at the spindle rotational frequency also introduce an undesirable low frequency forced vibration to the system, resulting in poor surface finish on the workpiece.

In a multi-tooth face milling system, two types of runout may occur. They are the radial throw and the axial throw. Radial throw occurs if not all insert cutting edges lie on the surface of a cylinder whose axis is perpendicular to the workpiece surface. Axial throw will be obtained if not all insert tips lie on the same plane parallel to the workpiece surface (DeVor et al.,[1]). In most practical machining processes, the axial throw, being much smaller than the depth of cut, can be neglected. In this paper, only the radial runout is considered.

One way to solve the radial runout problem is to manually pre-adjust the positions of each insert to compensate for the static runout which arises from the geometric variations in the insert sizes, insert setting, or cutter body, or from the spindle axis and the cutter axis misalignment . However, in addition to being costly and time consuming, this procedure is ineffective in controlling dynamic runout which develops during the cutting process such as uneven tooth wears. This motivates the approach of in-process active compensation for radial runout.

It is possible to actively compensate for runout, by varying the spindle speed or the feed rate. Since the runout pattern repeats itself every spindle revolution, the spindle speed or feed rate must also be adjusted accordingly at the same rate. Most machine tool feed axis carry a large slide inertial load and cannot respond quickly enough for runout compensations unless an unconventional quick response feed axis is added. Most modern machine tools, however, use spindles directly coupled to low inertia brushless DC or AC motors which have relatively fast responses in varying speeds. In this paper, only speed variations by the use of a commercially available spindle/brushless DC motor system are considered.

To date, the literature on active control of machining forces is primarily focused on the control of average cutting forces and on feed rate adaptation to slow changes in such conditions as depth of cut, width of cut and material properties (Masory and Koren [2], Tomizuka et al.[3], Lauderbaugh and Ulsoy [4], Fussell and Srinivasan [5]). Quickly varying disturbances due to runout, however, are generally neglected. In an attempt to tackle this problem, Tsao et al.[6] studied in-process active control of spindle speed and/or feedrate for reducing the effect of radial runout on cutting forces. In their paper, the following assumptions were made:
(1) The face milling cutter had at most a single tooth engaged in cutting at any instant.
(2) The spindle drive dynamics were first order and there were no such realistic constraints as motor current or power limit.
(3) The cutting torque feedback to the motor drive was neglected in the model development and control system design.

This paper extends the previous work and is focused on the feasibility of implementation. New contributions of this paper includes the following:
(1) Multi-tooth engagement is considered, which is more usual than single-tooth engagement.
(2) Realistic high order motor drive dynamics with current saturation are derived and the model is experimentally validated.

(3) The cutting torque feedback to the motor drive is included in the model development and control system design. Without doing so, the system may be unstable in some cases.
(4) The controller design is refined to make the control system more robust to unmodeled dynamics.

The remainder of this paper is organized as follows. Section 2 derives the mathematic model for the face milling system, which includes the cutting dynamics and the spindle drive dynamics. Section 3 derives a simplified model based on which a digital control system is obtained to compensate for runout disturbances. Section 4 presents simulation results and discussions followed by the conclusions in Section 5.

FACE MILLING PROCESS MODEL

In this section we derive a dynamic model for the face milling process. The model contains two elements, the machining process and the spindle/motor drive dynamics, as shown in Figure 1. The figure clearly shows a feedback interaction between the machining process and the spindle/motor drive. In the sequel, the face milling force model is derived based on earlier work on tool path geometry(Martellotti [7] and [8], Sabberwal [9], Ber and Feldman [10]) and cutting force mechanistic model (Koenigsberger and Sabberwal [11], DeVor et al. [1], Klein and DeVor [12], Fu et al., [13]) and the motor/spindle drive dynamics are derived by a standard method and validated on an industrial DC brushless motor/spindle system.

Cutting Force Model

The face milling process can be depicted as shown in Figure 2. The cutter is mounted on a spindle and rotates at a speed w while being fed into the workpiece at a constant feed rate v_0. Replaceable inserts which remove material are mounted on the cutter.

Without loss of generality, assume that the the angle of the first insert equals to the cutter angle and the cutter angle is initially at zero. We write

$$\theta_i = \theta - (i-1)\cdot\Delta\theta, \quad i = 1,2,...,Nt, \tag{1}$$

where θ_i is the angle of i'th tooth, θ is the cutter angle, Nt is the cutter tooth number, and $\Delta\theta = 2\pi/Nt$ is the tooth spacing angle.

The tangential force generated on insert i at any instant may be related to the process parameters by the equation

$$\begin{aligned} Ft_i &= K_t \cdot d \cdot \tau(\theta_i) && \text{if engaged in cutting} \\ &= 0 && \text{if not engaged in cutting} \end{aligned} \tag{2}$$

where K_t is related to the cutting conditions and material properties, d is the depth of cut, and τ is the chip thickness. K_t is determined experimentally for various cutting conditions.

The chip thickness is a function of the feed rate and the spindle speed. If the radius of the cutter is much larger than the feed per tooth, it has been shown (Martellotti, [7]) that by geometrical consideration the chip thickness on insert i may be approximated by the equation

$$\tau(\theta_i) = f_t \cdot \sin(\theta_i), \tag{3}$$

where f_t is the feed per tooth, the distance that the spindle has moved between consecutive passes of the teeth at the angle θ_i.

The feed per tooth is related to the cutter position by

$$f_t(t) = x(\theta) - x(\theta-\Delta\theta), \tag{4}$$

where, $x(\theta)$ is the position of the cutter in the feed direction with respect to the workpiece. When radial runout exists, the chip thickness is

$$\tau(\theta_i) = f_t \cdot \sin(\theta_i) + \Delta_i, \tag{5}$$

where Δ_i represents the additive chip thickness disturbance on insert i due to radial runout. Δ_i is simply the difference between the effective radius of tooth i, which is engaged in cutting at an angle θ_i, and that of the previous tooth, $i-1$, when it was at angle θ_i. Δ_i repeats itself each revolution and is thus periodic.

Combining (4) and (5), we get the following expression for the chip thickness as a function of cutter position, insert angle and radial runout.

$$\tau(\theta_i) = (x(\theta) - x(\theta-\Delta\theta))\sin(\theta_i) + \Delta_i \tag{6}$$

The maximum tangential cutting force is defined as

$$\begin{aligned} Ft_{max} &= \max_{i=1...Nt} Ft_i \\ &= \max_{i=1...Nt} K_t \cdot d \cdot \{(x(\theta) - x(\theta-\Delta\theta))\sin(\theta_i) + \Delta_i\} \end{aligned} \tag{7}$$

and the resultant cutting torque applied to the cutter is

$$\begin{aligned} T_{cut} &= R \cdot \sum_{i=1}^{Nt} Ft_i \\ &= R \cdot K_t \cdot d \cdot \sum_{i=1}^{Nt} \{(x(\theta) - x(\theta-\Delta\theta))\sin(\theta_i) + \Delta_i\} \end{aligned} \tag{8}$$

Finally, the cutter position is dependent on the spindle speed and feed rate by the following equation

$$\frac{dx}{d\theta} = \frac{\frac{dx}{dt}}{\frac{d\theta}{dt}} = \frac{v(t)}{w(t)} = \frac{v(\theta)}{w(\theta)} \tag{9}$$

where θ is the total angle traveled by the cutter originally at 0° (see Fig. 2).

It is clear from equation (6) to (8) that the radial runout will cause uneven maximum tangential force and non-uniform cutting torque, and this effect can be eliminated by changing feedrate and/or spindle speed. In this paper, our goal is to regulate the peak tangential force at a specified value by varying the spindle speed.

It should also be noted that the face milling force model derived here is a nonlinear dynamic system, which uses cutter angle instead of time as its independent variable.

Motor/Spindle Drive Dynamics

We consider a face milling spindle coupled directly to a three phase brushless DC motor. Figure 3 shows a DC motor equivalent block diagram for the three phase brushless motor dynamics, where $F_{rw}(s)$ is the velocity loop controller; $F_{ri}(s)$ is the current loop PI controller and $F_g(s)$ is the tachometer dynamics. G_d represents the relation between the spindle speed and the cutting torque which feeds back to the spindle drive. G_d will be derived in the next section and is not considered in the derivation of the spindle drive dynamics. Using the numerical data of our laboratory setup listed in Table 1, the calculated frequency response from the current command input U_i^* to the tachometer velocity output W_a has been compared with experimental results with excellent agreement up to 70 Hz. as shown in Figure 4.

The velocity loop controller is a plug-in module which can be easily changed for different applications. We use a PI controller for the velocity loop. The transfer functions from the velocity command U_w^* and external torque T_{cut} to the spindle speed output w are

$$w = G_u(s)\, U_w^* - G_t(s)\, T_{cut}, \tag{10}$$

where the transfer functions can be calculated from the motor data in Table 1 and are both of fifth order. Note that the negative sign in the equation implies that the cutting torque is in the opposite direction to the spindle speed.

The motor/spindle dynamics in Equation (10) can be realized in the time domain by its state equation form

$$\frac{d\bar{x}}{dt} = [A]\bar{x} + [B]U_{w^*} + [D]T_{cut}$$
$$w = [C]\bar{x} \qquad (11)$$

It should be noted that the cutting torque in Eq. (8) is in terms of cutter angle while the drive dynamics in Eq. (11) is in terms of time. We need to convert the latter to angle domain for the convenience of computer simulation and control system design. Dividing both sides of (11) by w, we get the state equation for the drives in the angular domain.

$$\frac{d\bar{x}}{d\theta} = \frac{1}{w}\left\{[A]\bar{x} + [B]U_{w^*} + [D]T_{cut}\right\} \qquad (12)$$

Equations (7-9) and (12) comprise the complete model of the face milling process using cutter angle as the independent variable. This model is suitable for dynamic simulations of the face milling process and will be called the simulation model. The simulation model contains nonlinear, "time" varying and delay terms. The control system design, which is directly based on this model, is very difficult, if possible at all. In the next section a simplified model derived from the simulation model is obtained for the purpose of control system design. The simplified model will be called the control model.

CONTROL SYSTEM DESIGN

Simplified Linear Continuous Model

Equation (8) is first simplified by assuming that the number of teeth approaches infinity. In this case we have

$$T_{cut} = \lim_{i\to\infty} R\cdot K_t\cdot d\cdot \sum_{i=1}^{Nt}\{\,(x(\theta) - x(\theta-\Delta\theta))\sin(\theta_i) + \Delta_i\}$$

$$= R\cdot K_t\cdot d\cdot \frac{dx}{d\theta}\cdot\left(\int_{\alpha_{in}}^{\alpha_{out}} \sin\phi\, d\phi + \int_{\alpha_{in}}^{\alpha_{out}} \frac{dR}{d\phi}\, d\phi\right)$$

$$= R\cdot K_t\cdot d\cdot (\cos\alpha_{in} - \cos\alpha_{out})\frac{v_o}{w} + \text{periodic disturbances} \qquad (13)$$

where α_{in} is the entry angle and α_{out} is the exit angle of the cutting inserts. Equation (13) shows a static but nonlinear relation between spindle speed w and the cutting torque T_{cut}. The disturbance input term will be dropped hereafter since the controller design only requires the transfer function from the control input to the output variable. By linearizing (13) around a nominal speed w_o we get

$$\delta T_{cut} = G_d\,\delta w, \quad G_d = -R\cdot K_t\cdot d\cdot(\cos\alpha_{in} - \cos\alpha_{out})\cdot\frac{v_o}{w_o^2}, \qquad (14)$$

where δ represents the variations from the nominal values.

Next, Equation (12) is linearized around the nominal speed w_o. Denoting σ as the Laplace transform variable of the cutter angle θ, we can derive the linearized model of Eq. (12) in transfer function form:

$$\delta w = G_u(w_o\,\sigma)\,\delta U_{w^*} - G_t(w_o\,\sigma)\,\delta T_{cut} \qquad (15)$$

The transfer functions are obtained from replacing s by $w_o\sigma$ in Eq. (10).

Combining (14) and (15) the transfer function from the speed command to the actual speed is

$$\delta w = G_p\,\delta U_{w^*}, \quad G_p = \frac{G_u}{1 + G_t G_d} \qquad (16)$$

Finally, in relating the maximum tangential force to the spindle speed using Eq. (7), we assume that the number of tooth is large and the runout is much smaller than the nominal feed per tooth so that Ft_{max} occurs at an insert whose angle is close to ninety degrees. Again, linearizing around w_o we get

$$\delta Ft_{max} = G_f\,\delta w, \qquad G_f = -K_t\cdot d\cdot\frac{v_o}{w_o^2}\cdot\frac{1 - e^{-\sigma\Delta\theta}}{\sigma} \qquad (17)$$

Therefore, the control model, which has the speed command as input and the maximum tangential force as output, is

$$\delta Ft_{max} = G_f G_p\,\delta U_{w^*} \qquad (18)$$

The variations δ in Equations (15) to (18) will be dropped hereafter for the convenience of presentation.

As will be verified by simulation, although the above derivation is based on the assumption that the cutter has a number of tooth approaching infinity, the robust feedback controller presented below will be able to control a cutter with as small as eight teeth.

Repetitive controller design

The control problem here is to regulate the maximum tangential force on all the cutting inserts to a desired value under the disturbances from the radial runout. Since any disturbance due to runout varies the peak force periodically, a repetitive controller is used here because it generates a periodic control signal to cancel the periodic disturbance. The detailed analysis of the stability and robustness of digital repetitive controller can be found in Tomizuka et al.[14]. A summary of the repetitive controller design follows.

Consider the feedback control system structure in Figure 5. Let the zero order hold equivalent discrete transfer function of the control model in Eq. (18) be of the following form:

$$G(z^{-1}) = \frac{Ft_{max}(z^{-1})}{U_{w^*}(z^{-1})} = \frac{z^{-d}B(z^{-1})}{A(z^{-1})} = \frac{z^{-d}B^+(z^{-1})B^-(z^{-1})}{A(z^{-1})}, \qquad (19)$$

where z^{-1} is a one step delay operator; d is the delay of the process and should not be confused with the depth of cut; $B^-(z^{-1})$ contains the zeros on or outside the unit circle and the undesirable ones in the unit circle; $B^+(z^{-1})$ contains the zeros which are not in $B^-(z^{-1})$. A stable transfer function which is an N step delayed approximate inverse of the process dynamics can be defined as follows:

$$\frac{R(z^{-1})}{S(z^{-1})} = \frac{z^{-N+d+nu}A(z^{-1})z^{-nu}B^-(z)}{B^+(z^{-1})b}, \qquad (20)$$

where N is chosen to be the number of sampling for one period of the disturbance; nu is the order of polynomial $B^-(z^{-1})$; $B^-(z)$ is with z substituted for z^{-1} in and b is a scalar and is defined as:

$$b \geq \max_{\omega\in[0,\pi]} |B^-(e^{-j\omega})|^2$$

The repetitive controller has the following form:

$$Gc(z^{-1}) = \frac{Ln\cdot R(z^{-1})}{S(z^{-1})(1-z^{-N})} \qquad (21)$$

Notice the term $(1-z^{-N})$ is in the denominator of the controller transfer function. This term can produce repetitive control signal.

Ln is the update rate of the repetitive controller called learning rate. It has been shown that the controller in (21) will be asymptotically stable and asymptotically rejecting periodic disturbance if $0 < Ln < 2$ (Tomizuka et al. [14]). It has also been shown (Tsao and Tomizuka [15]) that the above controller is not robust to unmodeled dynamics because of its high-gain feedback nature. To ensure robust stability, a modified repetitive controller has been proposed

$$Gc(z^{-1}) = \frac{Ln \cdot R(z^{-1})F(z^{-1})}{S(z^{-1})(1 - F(z^{-1})z^{-N})} \qquad (22)$$

where $F(z^{-1})$ is a low-pass filter. By reducing the feedback gain at high frequencies, the robust stability can be maintained while the high frequency disturbance rejection capability is sacrificed.

SIMULATION RESULTS

Since the repetitive controller in is designed based on the linearized control model, simulation on the comprehensive simulation model in Section 2 is necessary to justify the properness of the linear controller design and to evaluate the performance limitation under practical constraints.

Unless otherwise mentioned, the face milling process parameters are as follows:

Nt	= 8		(number of cutter inserts)
$diam$	= 0.10	m	(nominal cutter diameter)
wid	≥ 0.10	m	(workpiece width, immersed cutting)
w_O	= 200.	rpm	(nominal spindle speed)
d	= 1.23	mm	(depth of cut)
fpr	= 0.48	mm	(feed per revolution)
Δ_1	= 0.014142	mm	(runout disturbance as seen by insert 1)
Δ_2	= 0.0058579	mm	(runout disturbance as seen by insert 2)
Δ_3	= -0.0058579	mm	(runout disturbance as seen by insert 3)
Δ_4	= -0.014142	mm	(runout disturbance as seen by insert 4)
Δ_5	= -0.014142	mm	(runout disturbance as seen by insert 5)
Δ_6	= -0.0058579	mm	(runout disturbance as seen by insert 6)
Δ_7	= 0.0058579	mm	(runout disturbance as seen by insert 7)
Δ_8	= 0.014142	mm	(runout disturbance as seen by insert 8)
K_t	= 7.6332e8	N/m²	(K_t value for 390 Casting Aluminum under nominal feedrate and depth of cut)

Using Equation (18) and the motor/spindle data in Table 1, the angle domain linear continuous transfer function is found to be

$$G(\sigma) = \frac{Ft_{max}(\sigma)}{U_{w^*}(\sigma)} = \frac{-2.48e5(\sigma+239)(\sigma+119)(\sigma+4.10)(1-e^{-0.7855\sigma})}{\sigma(\sigma+856)(\sigma+329)(\sigma+118)(\sigma+.649\pm 2.6j)} \qquad (23)$$

The discrete transfer function with a sampling interval of nine degrees cutter rotation is found to be

$$G(z) = \frac{(z+1.154)(z-0.525)(z-2.46e\text{-}4)(z-1.22e\text{-}8)(z+8.34e\text{-}18)(z^4+z^3+z^2+z+1}{z^5(z-0.829\pm 0.359j)(z-9.16e\text{-}9)(z-1.65e\text{-}16)(z-7.412e\text{-}18)} \qquad (24)$$

By Equation (20) the repetitive controller is found to be

$$Gc(z^{-1}) = \frac{U_{w^*}(k)}{e(k)} = \frac{Ln \cdot z^{-39}F(z^{-1})(1.2z^5+.24z^4-.48z^3+.34z^2+.34z-.81+.1z^{-1}+.82z^{-2}-7.5e\text{-}9z^{-3}+1.3e\text{-}24z^{-4}-9.1e\text{-}42z^{-5})}{116(1-F(z^{-1})z^{-40})(-2.95+1.55z^{-1}-3.80e\text{-}4z^{-2}+4.62e\text{-}12z^{-3}+3.86e\text{-}29z^{-4})} \qquad (25)$$

where $F(z^{-1})$ is chosen as

$$F(z^{-1}) = \frac{z^2+4z+6+4z^{-1}+z^{-2}}{16} \qquad (26)$$

Six cases have been simulated to investigate the following considerations:

(1) Justification of the linear controller design and its effectiveness on radial runout compensation.
(2) The effects of the cutting torque feedback on the system stability.
(3) The effects of the digital filter on the robustness of the controller.
(4) The effects of different types of runout on the controller.
(5) The effects of high spindle speed.
(6) The effects of larger inserts number on the cutter.
The simulation results are discussed below.

Case 1. In this case the linear controller in Eq.(25) has been simulated on the default cutting condition and the results are shown in Figure 6. The cutter is engaged at the second cutter revolution without the repetitive controller being activated. It can be seen that the runout causes a substantial periodic peak force variation. The repetitive controller is then activated at the sixth cutter revolution. The maximum force variation is eliminated in about two cutter revolutions. This fast convergence indicates that the linear controller design is valid for the complicated milling process. The motor current varies about 6.5 Amperes from its nominal value (8 Amperes) in order to alter the spindle speed. The spindle speed varies about 5 rad/sec. (47.8 rpm.) from its nominal value at 20.944 rad/s (200 rpm.) in order to compensate for the radial runout.

It is interesting to observe the cutting torque and find that the controller, originally designed to regulate the maximum tangential force, is also controlling the cutting torque. When the controller is designed to control the cutting torque, we have observed that (the results are not shown here) the maximum tangential force is also under control. These observations indicate that it might be possible to indirectly control the maximum tangential force by controlling the cutting torque, whose on-line measurement is easier.

Case 2. The cutting torque feedback may affect the system stability and should be included in the controller design. Gd in Equation (16) is set to zero if the cutting torque feedback is neglected. By simulation results not shown here, it has been found that in light cutting condition such as that of Case 1, the control system is still stable even without considering the cutting torque feedback in the controller design. However, in heavier cutting condition, for example, the depth of cut is increased to 4.5 mm from 1.23 mm, the system becomes unstable if the cutting torque feedback is not considered in the controller design (see Figure 7b). In contrast, the control system that includes the cutting torque feedback Gd in the controller design remains stable and performs well (see Figure 7a). Same results have been observed for larger feed per tooth (0.25 mm) and harder materials ($K_t = 32 \times 10^8$).

Case 3. The low-pass filter, $F(z^{-1})$ increases the robust stability of the control system. A digital low-pass filter in Equation (26) has been used in all simulations because there are unmodeled dynamics due to the simplifications and linearizations done in deriving the control model. From simulation results not shown here, we have observed that the system is always unstable if the low-pass filter is not employed.

Case 4. If the runout is not a progressive one like that happens in spindle eccentricity, the controller designed for regulating the maximum tangential force may not be able to regulate the cutting torque at the same time and vise versa. With a random runout setting shown below, which is in contrast with the progressive type runout in Case 1, the simulation results in Figure 8 shows that the same controller used in Case 1 does regulate the maximum tangential force but is not able to regulate the cutting torque as a bonus. The much larger motor current variations compared with that of Case 1 are due to the larger runout setting and its randomness.

Δ_1	= 0.0000000	mm	(runout disturbance as seen by insert 1)
Δ_2	= 0.0000000	mm	(runout disturbance as seen by insert 2)
Δ_3	= 0.0000000	mm	(runout disturbance as seen by insert 3)
Δ_4	= 0.0143000	mm	(runout disturbance as seen by insert 4)
Δ_5	= 0.0037000	mm	(runout disturbance as seen by insert 5)
Δ_6	= 0.0200000	mm	(runout disturbance as seen by insert 6)
Δ_7	= -0.0092500	mm	(runout disturbance as seen by insert 7)
Δ_8	= -0.0287500	mm	(runout disturbance as seen by insert 8)

Case 5. The nominal spindle speed is limited by the maximum current available to the motor. Figure 9 and 10 show the simulation results of nominal speed at 500 rpm and 700 rpm, respectively. When the nominal spindle speed is 500 rpm, the armature current almost reaches its amplifier saturation (50A) after the repetitive controller is activated. When the armature current is saturated, the control system cannot work properly because the motor does not have enough power to alter the spindle speed, as is the case of 700 rpm. One way to solve this problem is to use a power amplifier and motor that allow larger excursion of the motor current.

Case 6. In this case, the cutter tooth number is increased to 24 while other cutting conditions remain the same as that of Case 1. The simulation results in Figure 11 show that the maximum tangential force is very smooth and the motor current variations are slight. This suggests that the method proposed here is even more suitable for large insert number situations.

CONCLUSIONS

We have successfully applied repetitive control algorithm to suppress the periodic cutting force variations caused by radial runout in face milling. The main feature of this digital control algorithm is that the sampling interval is in terms of cutter angle instead of the real-time. The design of an effective repetitive controller is not straightforward because the dynamics of both the spindle drive and the cutting process have to be considered. The cutting process model is so complex that, on one hand, it must be simplified and linearized to a form which can be useful to the control system design, but on the other hand, it must not be neglected in control system design because the unmodeled cutting torque feedback may be significant enough to make the control system unstable. Currently available digital signal processors should have more than enough real-time computation power to implement the control algorithm in this paper.

Our simulation results based on a commercially available DC brushless motor have shown that speed variation in every spindle rotation is possible at nominal speeds up to 500 rpm. This suggests that active runout compensation, achieved by varying the spindle speed, is feasible at least for situations where larger diameter cutters and hence lower nominal spindle speeds are used. The performance of modern electric drives may extend beyond what we have estimated from the simulation results in this paper. Brushless DC motors can have large torque to rotor inertia ratio. Pulse width modulated power amplifiers can have a high bandwidth current loop dynamics and allow large instantaneous peak currents. Power electronic devices which have the power regeneration feature are also energy efficient in accelerating and decelerating motors.

The implementation of the control system needs the feedback signal from the maximum tangential cutting force. In order to have this, the tangential force on every cutting insert must be measured on-line. This is not an easy task. We have shown that if the radial runout is of progressive type as is commonly encountered due to spindle or cutter eccentricity, control the cutting torque can also regulate the maximum tangential force. The cutting torque can be easily obtained by using a single torque transducer or by monitoring the motor current and speed. It is also possible to on-line estimate cutter runout by the measurement of resultant cutting torque or forces (Gu et al. [16]). The on-line measurement of individual tangential cutting force on each insert is also possible with the recent advances in micromechanical sensors and with the concept of intelligent insert (Ramalingam et al. [17]). An intelligent insert is an instrumented insert with an integral transducer element which is constructed by vacuum depositing a thin film transducer directly on the non-cutting face of an insert. However, the intelligent inserts are not commercially available yet.

ACKNOWLEDGEMENT

The authors gratefully acknowledge the University of Illinois Research Board for providing computer time for this research, Professor R. E. DeVor and Professor S. G. Kapoor of University of Illinois at Urbana-Champaign, for their encouragement and the access to their machining research equipment, and Mr. Erickson and Mr. Letellier of Indramat Division, Rexroth Corporation, for providing the motor parameters.

REFERENCES

[1] DeVor, R.E.,Kapoor,S.G., Fu, H.J. and Subbarao, P.C., "Effect of Variable Chip Load on Machining Performance in Face Milling," Proceedings of the 11th North American Manufacturing Research Conference, May 1983, p.348

[2] Masory, O., and Koren Y.," Adaptive Control System for Turning," CIRP Ann., vol. 29, no.1 pp.281-284, 1980

[3] Tomizuka, M.,Oh, J. H., and Dornfeld, D. A.,"Model Reference Adaptive Control of the Milling Process," Proceedings of the Symposium on Manufacturing Processes and Robotic Systems, p.55, ASME Winter Annual Meeting, New York, November, 1983

[4] Lauderbaugh, L.K., and Ulsoy, A.G., "Model Reference Adaptive Force Control in Milling," Proceedings of the Symposium on Modelling, Sensing and Control of Manufacturing Processes, ASME Winter Annual Meeting, PED vol.23, p.165, 1986

[5] Fussell, B.K., and Srinivasan, K., "Adaptive Control of Forces in End Milling Operations - An Evaluation of Available Algorithms," ASME Journal of Manufacturing Systems, April, 1988

[6] Tsao,T., Burke, J. B. ,Ferreira, P.M., "Control of Radial Runout in Face Milling," Symposium on Control Issues in Manufacturing Processes, ASME, 1989

[7] Martellotti, M.E., "An Analysis for the Milling Process," Trans. ASME, vol. 63, 1941, p.667

[8] Martellotti, M.E., "An Analysis of the Milling Process, Part II: Down Milling," Trans. ASME, vol. 67, 1945, p.233

[9] Sabberwal, A.J.P.,"Chip Section and Cutting Force During the Milling Operation,"Annals of CIRP 1960

[10] Ber A. and Feldman D., "A Mathematical Model of the Radial and Axial Throw of Square Indexable Inserts in a Face Milling Cutter," Annals of CIRP 1976

[11] Koenigsberger, F., and Sabberwal, A.J.P., "An Investigation Into the Cutting Force Pulsations During Milling Operations," Int. J. Mach. Tool Des. Res., vol, 1961, p.15

[12] Kline, W.A., and R.E. DeVor, " The effect of Runout on Cutting Geometry and Forces in End Milling," Int. Jour. Mach. Tool Des. and Res., vol. 23, no. 2,1983, pp.123-140

[13] Fu, H.J., DeVor, R.E., Kapoor, S.G., "A Mechanistic Model for the Prediction of the Force System in Face Milling Operations," Journal of Engineering for Industrial Trans. ASME, 1984, vol.106, No1, p81-88

[14] Tomizuka, M., Tsao, T., and Chew, K., "Discrete Time Domain Analysis and Synthesis of Repetitive Controller," Proc. of the 1988 American Control Conference, June, 1988

[15] Tsao,T.,Tomizuka,M.,"Adaptive and Repetitive Digital Control Algorithms for Noncircular Machining"Proc. of the 1988 American Control Conference,1988,p115-120

[16] Gu,F.,Kapoor,S.G.,DeVor,R.E., "An Approach to On-line Runout Estimation in Face Milling," submitted to North American Manufacturing Research Conference, May 1991

[17] Ramalingam, S.,Shi,T.,Frohrib, A. and Moser, T.,"Acoustic Emission Sensing With an Intelligent Insert and Tool Fracture Detection in Multi-tooth Milling," 16th North American Manufacturing Research Conference Proceeding, May 1988, p245

Name of Components	Parameters	Constants	Transfer Functions
Equivalent DC Brushless Spindle Drive	B J L_a R_a	0.02158 kgm^2/s 0.04041 kgm^2 0.0063 H 0.45 Ω	$\frac{1}{Js+B}$ $\frac{1}{L_a s+R_a}$
Torque Constant	Cwl	0.91 Nm/A	
Back e.m.f.	Cw2	0.91 Vs/rad	
Tacho Gain	Cwt	0.0286 Vs	
Tachometer Dynamic Fg(s)	T_g	0.0004 s	$\frac{1}{T_g s+1}$
Velocity Loop Controller Frw(s)	K_{pw} K_{iw}	2.805 V/V 241.0 s^{-1}	$\frac{K_{pw}s+K_{iw}}{s}$
Current Feedback	K_i	0.05 V/A	
Cur. Loop Gain	K_u	13.0 V/V	
Current Loop Controller Fri(s)	K_{pi} K_{ii}	240. V/V 1200000.s^{-1}	$\frac{K_{pi}s+K_{ii}}{s}$
Current Limit	ia(max)	50 A	

Table 1: Motor Drive Parameters

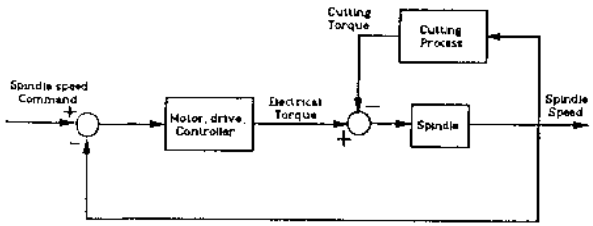

Figure 1: Schematics of the Face Milling Process

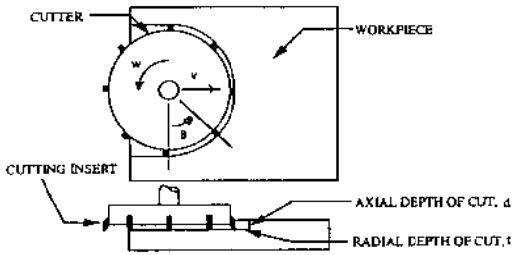

Figure 2: Geometry of Face Milling Process

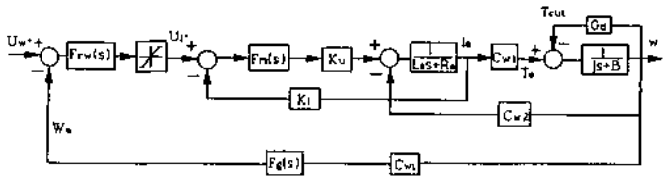

Figure 3: Block Diagram of the Spindle/Motor Dynamics

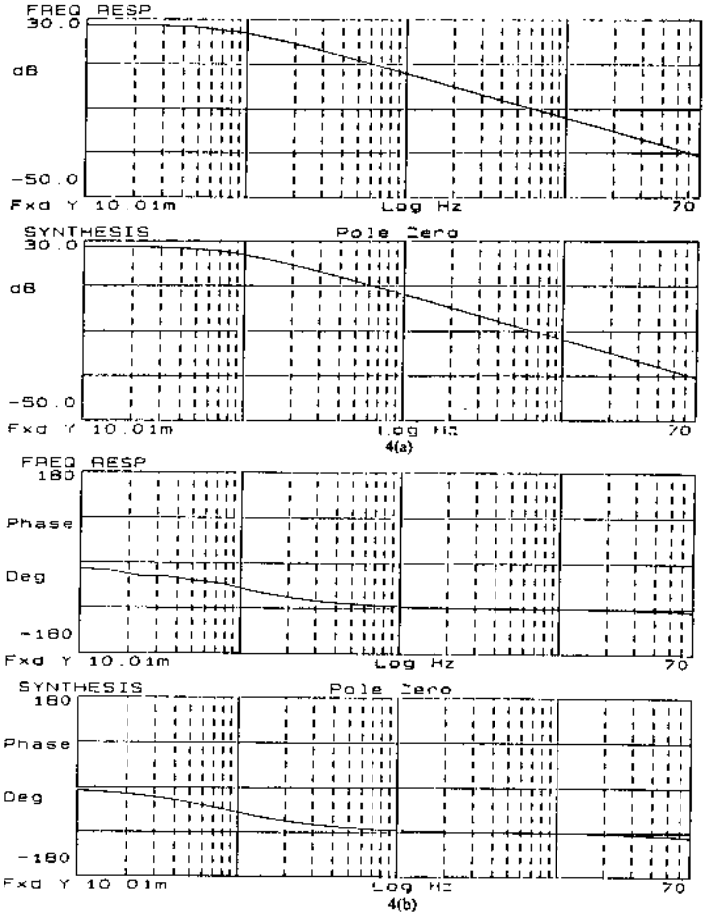

Figure 4: Frequency Responses of the Spindle/Motor Drive. 4(a) is the gain and 4(b) is the phase diagrams. The upper ones are from experiment and the lower ones are from the linear model.

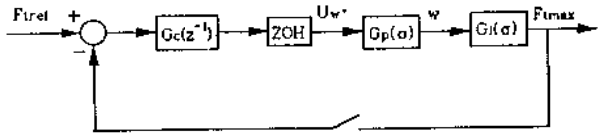

Figure 5: Block Diagram of the Digital Control System

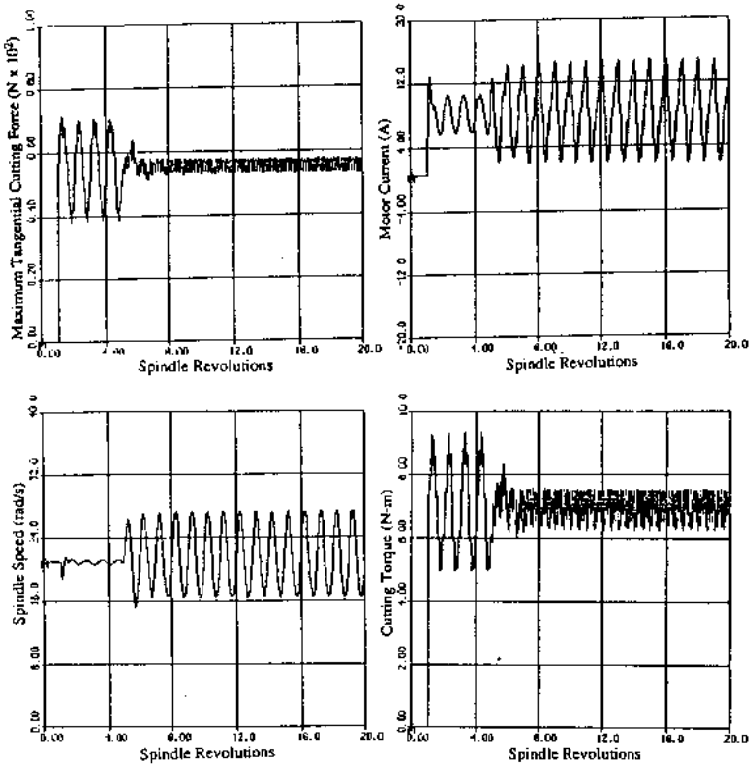

Figure 6: Simulation results with a progressive type of runout and with the default cutting conditions

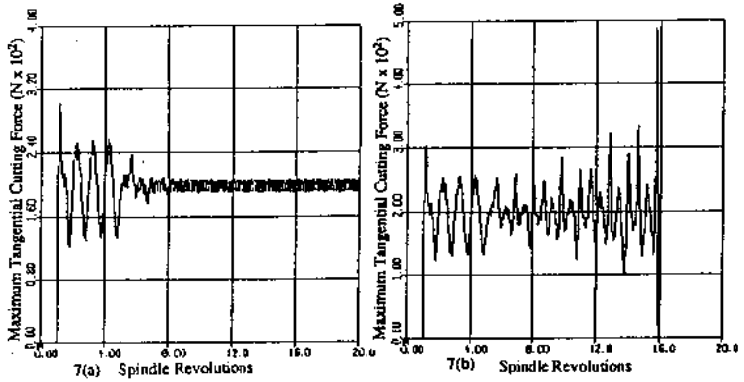

Figure 7: Simulation results with a large depth of cut. 7(a) has included the cutting torque feedback in the model for controller design. 7(b) does not include cutting torque feedback in the model for controller design.

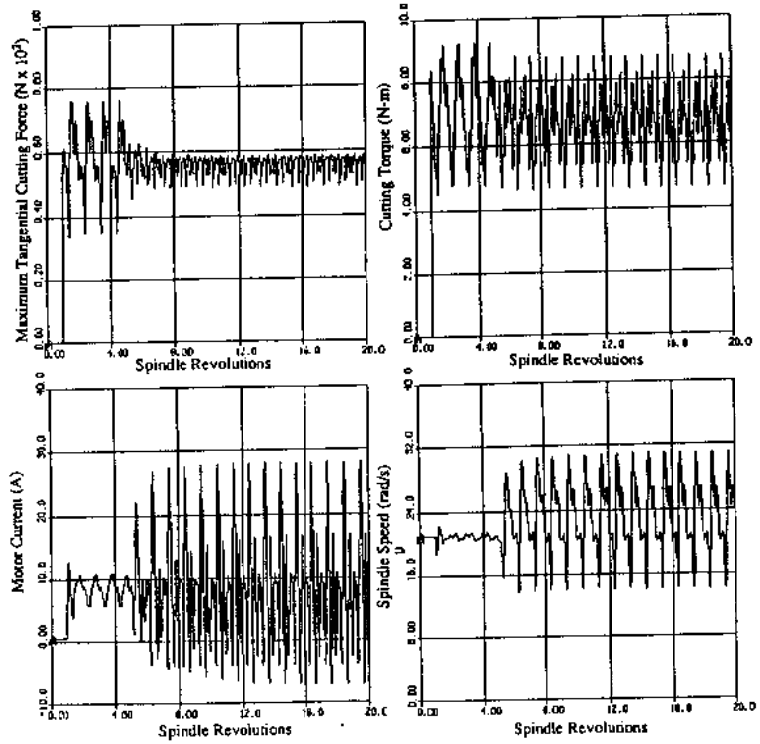

Figure 8: Simulation results with a random type of runout

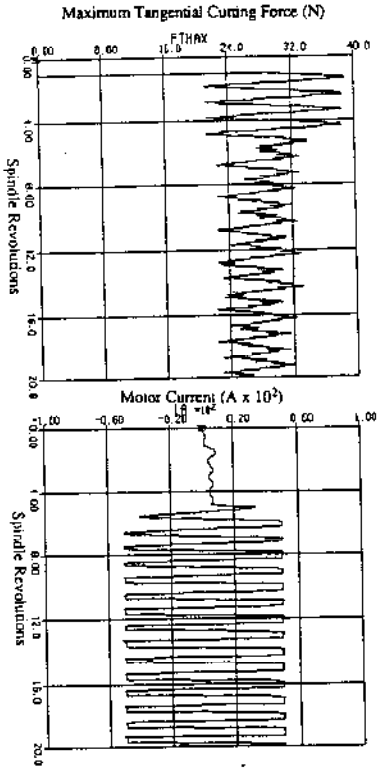

Figure 10: Simulation results with the nominal speed at 700 rpm

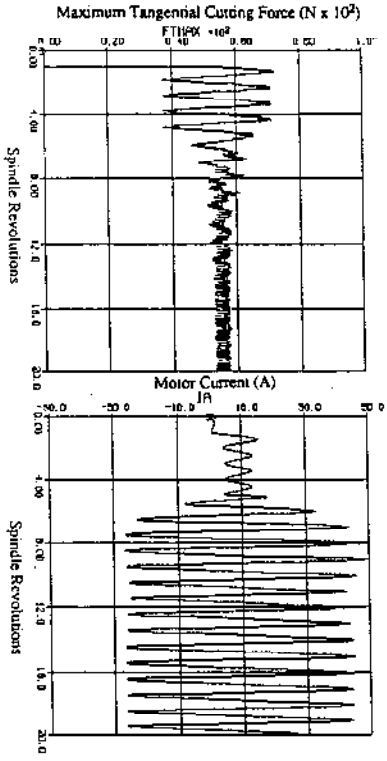

Figure 9: Simulation results with the nominal speed at 500 rpm

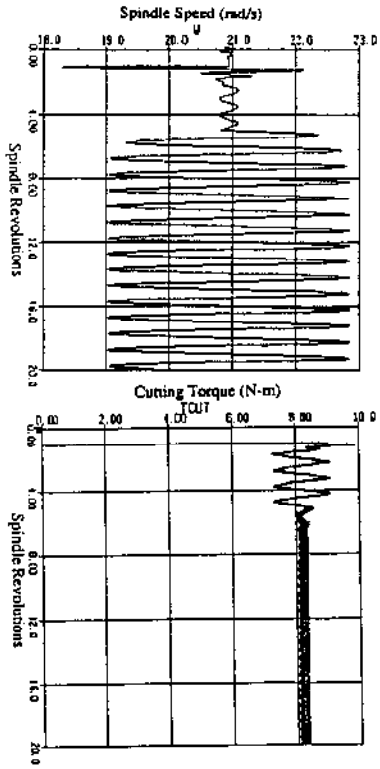

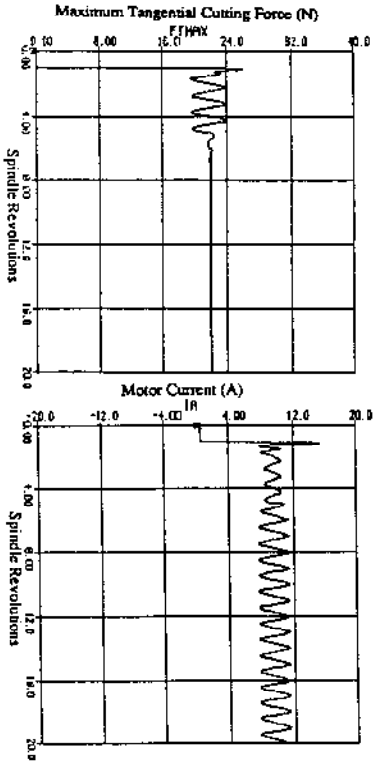

Figure 11: Simulation results with a 24 tooth cutter